Published online June 28, 2006

Nucleic Acids Research, 2006, Vol. 34, No. 11 ***e77***
doi:10.1093/nar/gkl416

Ultra fast miniaturized real-time PCR: 40 cycles in less than six minutes

Pavel Neuzil*, Chunyan Zhang, Juergen Pipper, Sharon Oh and Lang Zhuo

Institute of Bioengineering and Nanotechnology, 31 Biopolis Way, The Nanos, #04-01, Singapore 138669

Received March 9, 2006; Revised April 28, 2006; Accepted May 24, 2006

ABSTRACT

We have designed, fabricated and tested a real-time PCR chip capable of conducting one thermal cycle in 8.5 s. This corresponds to 40 cycles of PCR in 5 min and 40 s. The PCR system was made of silicon micromachined into the shape of a cantilever terminated with a disc. The thin film heater and a temperature sensor were placed on the disc perimeter. Due to the system's thermal constant of 0.27 s, we have achieved a heating rate of 175°C s^{-1} and a cooling rate of −125°C s^{-1}. A PCR sample encapsulated with mineral oil was dispensed onto a glass cover slip placed on the silicon disc. The PCR cycle time was then determined by heat transfer through the glass, which took only 0.5 s. A real-time PCR sample with a volume of 100 nl was tested using a FAM probe. As the single PCR device occupied an area of only a few square millimeters, devices could be combined into a parallel system to increase throughput.

INTRODUCTION

Since its invention (1) in 1985, the PCR has become a well-established method for amplification of segments of double-stranded DNA (2). Later on, Mullis employed a thermally stable polymerase (3) in order to avoid having to add polymerase to the PCR during the thermocycling process. That idea made the PCR technique available to molecular biologists.

A typical PCR process consists of three steps conducted at different temperatures: denaturation at 95°C, annealing at 50°C and extension at 72°C. Sometimes the annealing and extension steps are combined into one and performed at a temperature of about 60°C (Applied Biosystems: Essentials of Real-time PCR, http://www.appliedbiosystems.com/support/tutorials/pdf/essentials_of_real_time_pcr.pdf) It is desired that the transition time between different temperatures should be as short as possible to avoid formation of non-specific byproducts and to reduce the thermal stress on the polymerase. The end-point PCR product can be confirmed by agarose gel electrophoresis or more recently, by capillary electrophoresis (CE) (4), when the PCR cycles are completed. However, an end-point measurement, which often happens in the plateau phase of a PCR, does not correlate well with the original amount of gene of interest. Real-time PCR, on the other end, monitors the PCR *in situ* by fluorescence arising from fluorogenic compounds (such as Taqman probe) or DNA intercalators (such as SYBR Green) incorporated in the PCR process, and allows precise quantitative information extracted from the exponential phase of the reaction (5,6). Taqman probe-based assay format, e.g. FAM™ (fluorophore) and TAMRA™ (quencher) labeled probe, is specific to its target gene, whereas SYBR Green-based format is non-specific. To determine the specificity of PCR product using SYBR Green, a subsequent melting curve analysis (MCA) (7,8) has to be implemented. The MCA is often preferred over CE as the MCA is performed in the PCR system simply by software modification.

The most popular PCR systems are based on Peltier element technology. A 96- or 384-well plastic PCR plate is thermally cycled in a heating block made of thermal conductive metals and the reaction volume is between 10 and 50 µl. Therefore, to ensure temperature homogeneity across the whole plate, a large value of thermal capacitance of the system is required. As the heating/cooling rates are functions of heat capacitance, conventional PCR systems are slow, with heating/cooling rates of a few °C per second. The speed can be improved either by increasing the rate of heat transfer or by decreasing the system's heat capacitance (heater and PCR sample volume). The shrinking of sample volume is an attractive option because it is faster as it enhances heat transfer and thermal equilibration and it is also cost-effective as it reduces the reagent amount. With the advent of micromachining (9) and its use in biological applications (10), a number of researchers have gotten involved in the development of micro PCR systems (11). Micromachining has enabled the handling and processing of samples in volumes as small as a few nano liters, either by cycling a stationary sample (12) at three different temperatures, or by moving a sample through/over three different temperature zones (13,14). In the past decade, researchers have dedicated great efforts to improve the speed and performance of PCR (15). For most of the studies, resistive heating or thermoelectric modules are used for thermocycling.

*To whom correspondence should be addressed. Email: pneuzil@ibn.a-star.edu.sg

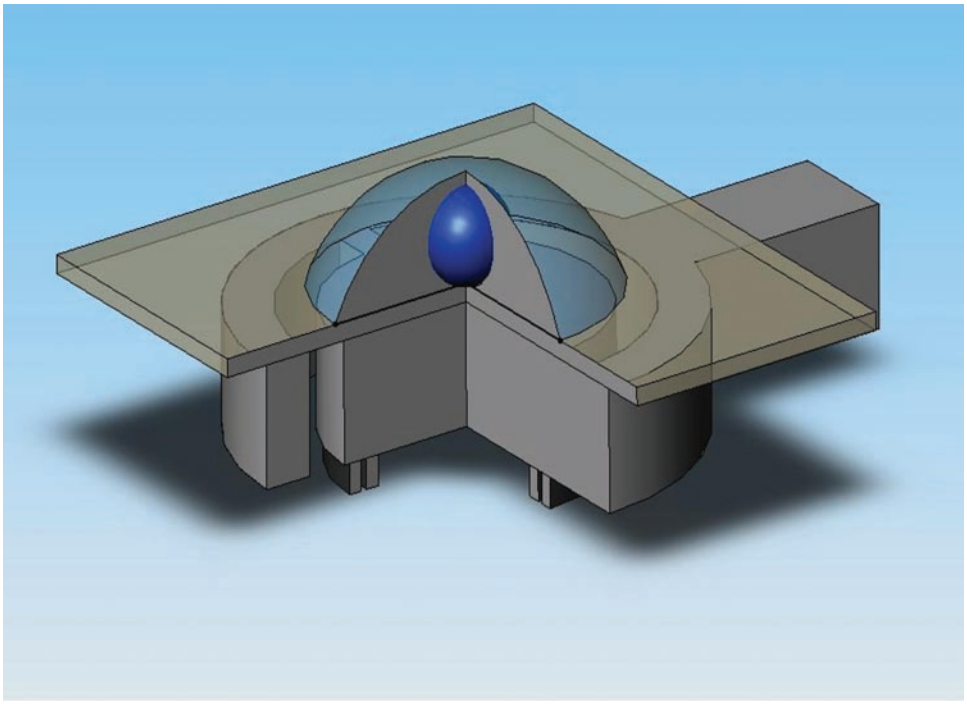

Figure 1. Schematic image of the proposed system made by silicon micromachining. It consists of an inner disc with a heater and a temperature sensor on the backside, connected by two narrow beams to an outer silicon ring. This ring is connected to the substrate by a cantilever. The sample (represented by a blue sphere) is covered by mineral oil and is placed on a glass microscope cover slip. The oil prevents water evaporation from the sample.

The heat transfer from the heater to the sample is a limiting factor for fast systems. Using infrared (IR) radiation as heat source at a wavelength only specific for water (H_2O) (16) provided an elegant solution, because the IR energy is only absorbed by the aqueous PCR sample [λ_{max} (H_2O) $\sim$1083 nm], but not by the surrounding material. A miniaturized 1248-well PCR platform was recently demonstrated (17). In this study, all wells were filled with mineral oil to prevent the samples from evaporation. Moreover, all the 1248-wells were thermally connected to ensure identical temperature for all the samples.

In this paper, we report on an ultra-fast real-time PCR system. It runs one thermal cycle in 8.5 s or one complete 40-cycle PCR protocol in 5 min and 40 s. The current set-up is based on one well. However, more wells can be integrated to form an array to cater for high-throughput applications.

THEORY AND EXPERIMENTAL

Theory

As described previously (18), good temperature control and uniformity within the silicon-based micro machined system was achieved by a double donut shape. The internal silicon donut was connected to the external one by two narrow silicon bridges, distributing the heat uniformly. The external donut in turn was connected to a silicon frame kept at room temperature by a cantilever.

Here, we propose replacing the inner donut with a solid disk (see Figure 1) and scaling the device size down by a factor of 2.

Let us consider that the PCR system is subject to dissipated power (Joule heat) of amplitude of P_H. The PCR temperature is given by the differential heat balance equation: (19)

$$H\frac{d\Delta T}{dt} + G\Delta T = P_H, \quad \mathbf{1}$$

where, H is the PCR heat capacitance, ΔT is the temperature change due to dissipated Joule heat P_H and G is the PCR thermal conductance. Thermal heat capacitance is essentially given by the combined heat capacity of the silicon disc and the sample. The thermal conductance is given by the formula

$$G = \frac{wt}{l}\lambda, \quad \mathbf{2}$$

where, w is the beam width, t is its thickness, l is its length and λ is the thermal conductance of silicon. The system's thermal time constant τ is then given by the equation

$$\tau = G/H. \quad \mathbf{3}$$

The PCR cooling rate is entirely determined by the time-constant while the heating rate is also determined by the amount of dissipated power.

Fast responding systems require a low value of thermal capacitance H and high thermal conductance G. However, as can be seen from Equation 1, in a steady-state ($G\Delta T = P_H$), the high value of G results in a power-demanding system.

The same effect could be achieved by lowering the system's thermal capacitance H using a smaller sample volume, while maintaining thermal uniformity. Silicon as a structural material has both high thermal conductivity as

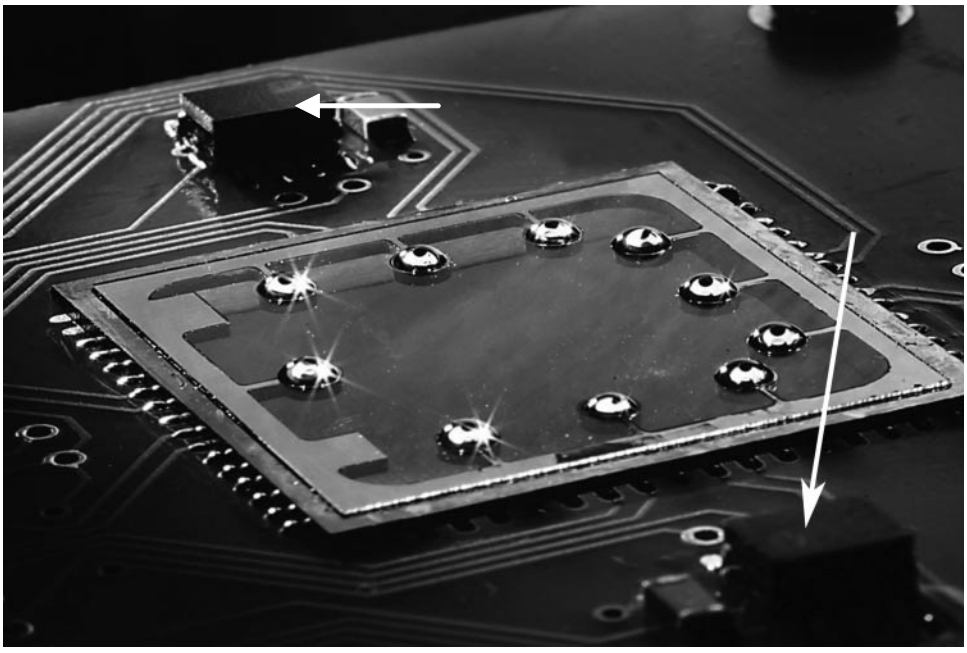

Figure 2. Microphotograph of a fabricated chip 24.2 × 24.2 mm in size, soldered to a PCB. The chip consists of 10 individually controlled heaters, which can run 10 PCRs simultaneously. The PCR mixture with a volume of 100 nl is surrounded by 1.1 μl of M5904 mineral oil (Sigma–Aldrich, Inc.) to prevent PCR sample evaporation. Two temperature sensors TSiC™ (IST A.G.) pointed by arrows in the SOIC-8 package are calibrated with a precision of ±0.05°C. They were used to calibrate the PCR chip temperature sensors.

well as mechanical strength. Comparing Equation 2 for the full size (18) and scaled models (used in this work), the thermal conductance would not change because changing the length l by a factor of 2 is compensated by changing the width w by the same factor. On the other hand, the value H will be decreased by the square of scaling factor as the thermal capacitance is function of an area of the donut resulting in a shorter thermal constant (see Equation 3), i.e. a faster system.

PCR fabrication

Double side-polished silicon wafers 100 mm in diameter were used as a substrate. First, the top surface of the wafers was covered by an electrically insulating silicon oxide (SiO_2) layer with a thickness of 500 nm, deposited by plasma-enhanced chemical vapor deposition (PECVD). Next, a 5 nm thick adhesion layer of chrome, followed by a 250 nm thick gold layer was deposited by electron beam evaporation for heaters, sensors and electrical connections to the bonding pads. The total sheet resistance of the metal sandwich was 0.11Ω/□.

Both metals were lithographically patterned using AZ7220 positive photoresist (Clariant, Inc.) with a thickness of 2 μm. Subsequently, metal etching was performed by reverse sputtering in an LLS EVO (Unaxis A.G.) system at an argon pressure of 400 mTorr and a total power of 200 W. The low plasma power during the reverse sputtering guaranteed that the photoresist did not get overheated during the etching process and could be removed by usual solvent.

After photoresist removal by acetone, the second lithography step was performed at the front side of the wafer using 10 μm thick AZ9260 photoresist (Clariant, Inc.). The silicon oxide was first etched by buffered oxide etch (BOE) solution consisting of seven parts of 40% NH_4F and 1 part of 49% HF and the silicon was subsequently etched through the entire wafer by the deep reactive ion etching (DRIE) Bosch process (20). As described in previous work (18), the scribe lines were also patterned, thus eliminating the dicing saw step of fragile wafers as they were singled by the deep DRIE process. Fabricated chips (see Figure 2) were individually cleaned in acetone, rinsed in de-ionized (DI) water and dried by flow of nitrogen.

Device characterization

Once fabricated, the devices were soldered to a printed circuit board (PCB) in order to enhance their mechanical strength and to form convenient electrical connections to them. This PCB was connected to another PCB to interface the PCR chip with a LabView Data Acquisition (DAQ) card (National Instruments, Inc.) controlled by a Personal Computer (PC). The second PCB contained an AC biased Wheatstone bridge to determine the PCR chip temperature with subsequent signal processing. Besides the bridge, there was also a power converter. It transforms low power pulse width modulated (PWM) signals generated by a PC to higher power pulses required for the PCR heater. During the PCR operation, the temperature profile was controlled by LabView software using a proportional integrated derivative (PID) method.

To calibrate the PCR chip, the whole PCR board was immersed into a bath filled with Fluorinert™ Electronic Liquid FC-70 (3 M Specialty Chemicals Division, Inc.), and the temperature was raised from 50 to 100°C. The output of the Wheatstone bridge was then recorded as a function of the bath temperature, measured with a precision of ±0.05°C by a TSiC™ (IST AG) proportional to absolute temperature

Table 1. Electrical and thermal parameters of the nanoPCR device itself

Sensor resistance (at 25°C)	427Ω
Heater resistance (at 25°C)	141Ω
System temperature response	11 mV/°C
PCR thermal conductance	0.42 mW/°C
PCR thermal capacitance	1.5 mJ/°C
PCR thermal time constant	0.28 s
Heating rate from 60 to 95°C	175°C/s
Cooling rate from 95 to 60°C	−125°C/s

(PTAT) type of sensor integrated onto the PCR board. After calibration of the PCR chip temperature sensor, a step function was applied to the heater. From the temperature response, the thermal time constant τ was derived as well as the PCR thermal G and the capacitance H. All measured and calculated values are listed in Table 1.

PCR setup

A glass cover slip with a thickness of about 170 μm was fluorinated by a chemical vapor deposition (CVD) process using a siloxane precursor (18) and placed on the silicon heaters. Due to the surface treatment, the glass was both hydrophobic and oleophobic. The average water contact angle using the sessile drop method was found to be 110 ± 2°, while the contact angle with mineral oil was 70 ± 2°. The quality of the surface treatment can be checked by immersion into ethanol. A perfect fluorinated surface is not wettable after being dipped and withdrawn from the ethanol solution. Following this procedure we have found the glass surface not being wettable, thus confirming the quality of the coating.

A total of 1.1 μl of M5904 mineral oil (Sigma–Aldrich, Inc.) followed by 100 nl of PCR mixture (see Figure 3) were manually dispensed onto the glass cover slip just above the silicon heater using an Eppendorf® Research Series 2100 Pipette with an adjustable volume from 0.1 to 2.5 μl (Eppendorf AG).

We chose 100 nl as the sample volume, because it is the smallest volume that can be handled by a manual pipette. The surface coating on the glass prevented both the mineral oil and the PCR mixture from spreading uncontrollably on the glass surface. The droplet was then placed under an Axiotech vario microscope (Zeiss, Inc.) equipped with a fluorescein isothiocyanate (FITC) filter set. An X-Cite 120 PC (EXPO Photonic Solution, Inc.) 120 W metal halide short arc lamp was used as a light source and a H5784-20 photo multiplier tube (PMT) (Hamamatsu Photonics K.K.) with the gain set to about 10^4 as the detector. The PMT output and the temperature signal were recorded simultaneously.

Sample preparation

The PCR mixture was prepared in a 0.2 ml PCR tube by mixing 5 μl of Taqman Fast Universal PCR Master Mix 2× (#4352042, Applied Biosystems, Inc.), 0.5 μl of Taqman Assays-by-Design (Applied Biosystems, Inc.) containing primers and probe encoding for the green fluorescent protein (GFP) gene (forward primer 5′-CACATGAAGCAGCACGACTT-3′; reverse primer 5′-CGTCGTCCTTGAAGAAGATGGT-3′, probe 5′-FAM-CATGCCCGAAGGCTAC-BHQ-1-3′), 2.5 μl of DI water and 2 μl of cDNA converted from total RNA of brain tissue from transgenic GFAP–GFP mice (21) by random hexamer priming using Taqman's reverse transcription (RT) reagent (#N808-0234, Applied Biosystems, Inc.). The length of amplicon was 82 bp.

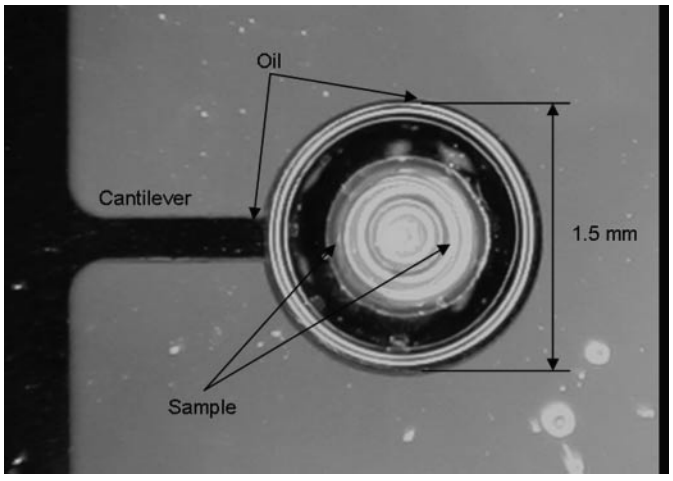

Figure 3. Optical photograph of the sample encapsulated by oil (edges pointed to by arrows) placed above the heater and separated from it by a microscope cover slip. The hemispherical oil shape formed a lens which magnified the sample.

Real-time PCR optimization

The recommended PCR thermal protocol optimized for the ABI 7500 Fast Real-time PCR system (Applied Biosystems, Inc.) consisted of a hot start by heating the PCR solution to 95°C for 20 s, followed by 40 cycles of denaturation at 95°C for 3 s and annealing/extension at 60°C for 30 s (see a typical thermal and fluorescence profile in Figure 4). The total time of running this protocol on our system is 27 min. What is the limitation of the individual steps? How short can the denaturation and annealing/elongation be, without affecting the efficiency of the PCR? First, 20 s at 95°C (hot start) is required to activate the enzyme, to melt away secondary structures, and to denature the full-length cDNA template, which was obtained by RT of RNA using random hexamers. What about the subsequent PCR steps? Denaturation of a significant portion of a DNA fragment is accomplished at temperatures above 90°C. Since this process is fast, the step duration using a commercially available thermocycler is dominated by the heating/cooling rate of the thermocycler.

As shown earlier (19) by solving Equation 1, the sample's temperature change is a function of heat transfer to the sample (12), together with the sample heat capacity. The temperature change can be increased by increasing the amount of power dissipated into the sample (for heating) as well as increasing the thermal conductivity G (for cooling). The sample heat capacity can be minimized by lowering the sample volume.

The PCR system described in this paper has a temperature sensor integrated in the vicinity of the heater at a distance of a few micrometers. In an equilibrium state, neglecting the vertical temperature gradient, the sensor will be subject to the same temperature as the average temperature of the

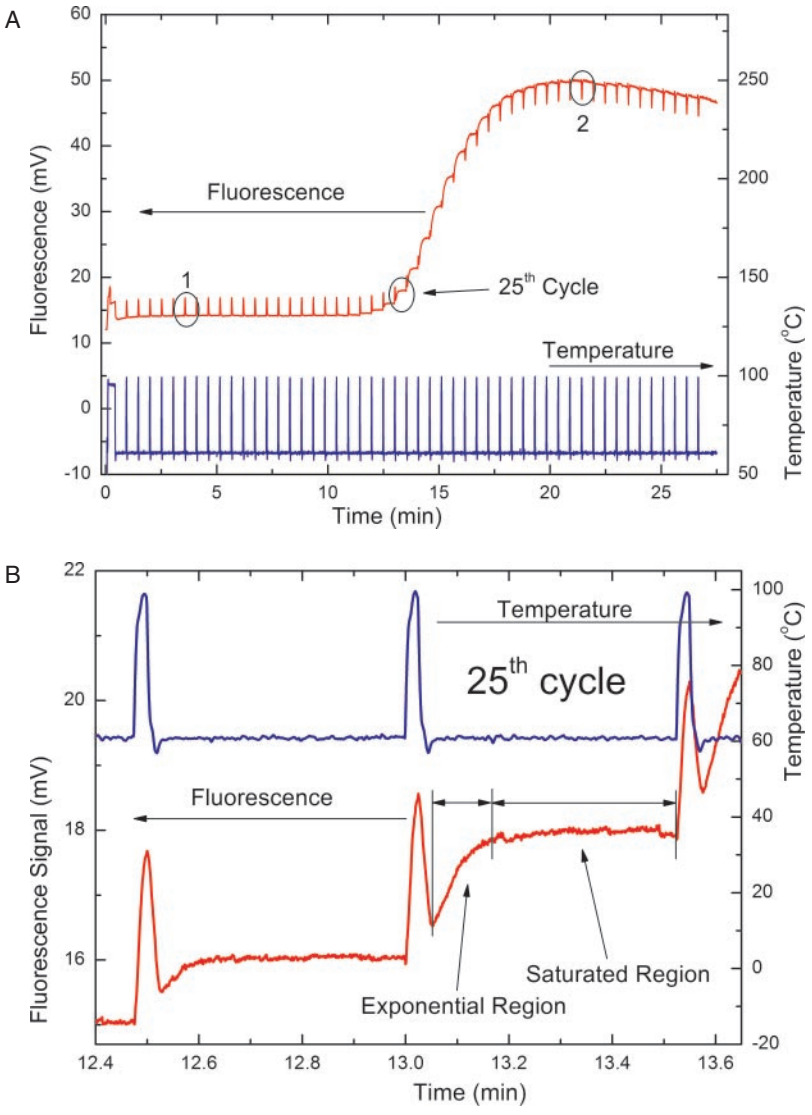

Figure 4. A typical real-time PCR curve showing the PCR thermal profile (blue) and fluorescence signal (red) for a complete 50 cycle PCR (upper figure). The critical threshold (C_T) was determined by plotting the mean value of the fluorescence signal of the last 5 s at each cycle versus cycle number on a logarithmic scale. We have found that the C_T value was 20.7. The fluorescence signal versus temperature graph shows a typical trend for a FAM probe-based system. At the beginning of the PCR cycling, the fluorescence increases with the temperature (1) while after successful PCR amplification shows the opposite trend (2). The fluorescence as well as the temperature signals detected within the 24th and the 25th thermal cycles are also shown (lower figure). The fluorescence signal within each step consists of two regions, one exponential and the other saturated (indicated by arrows). Within the 25th cycle the saturated part of the fluorescence signal is three times longer than the exponential part. The significance of this finding will be discussed later.

PCR sample. The problem is that the heater temperature is not necessarily identical to the temperature of the PCR solution. The question remains as to how to determine the PCR sample transient temperature during PCR cycling.

In a conventional PCR system the temperature sensor should be placed inside the PCR sample. It is a rather challenging task for the sample volume of 100 nl used in this experiment unless one uses focused laser light for temperature measurement.

In a real-time PCR system the fluorescent light is generated within the sample and detected by a light sensor, such as PMT. A method of temperature measurement of a sample using fluorescence was described earlier (22). Is it possible to take advantage of the natural temperature sensitivity of the PCR solution? A SYBR Green-based system emits the fluorescent signal by intercalation of SYBR Green into double-stranded DNA.

A probe-based system (such as 6-FAM) generates the fluorescent light by cleaving the covalent bond between the donor and acceptor dye. The cleaving is accomplished by exonuclease activity of Taq protein. The dye is then released, which increases the amplitude of the fluorescence signal.

In both cases the amplitude of the fluorescent signal is related to the sample temperature and the sample composition. It can then be used to monitor the transient sample temperature. The MCA method routinely conducted with SYBR Green-based systems can be used for PCR sample temperature monitoring. However, it can be used with high precision only around the melting point (8). We have tested the temperature sensitivity of the FAM based system and have found

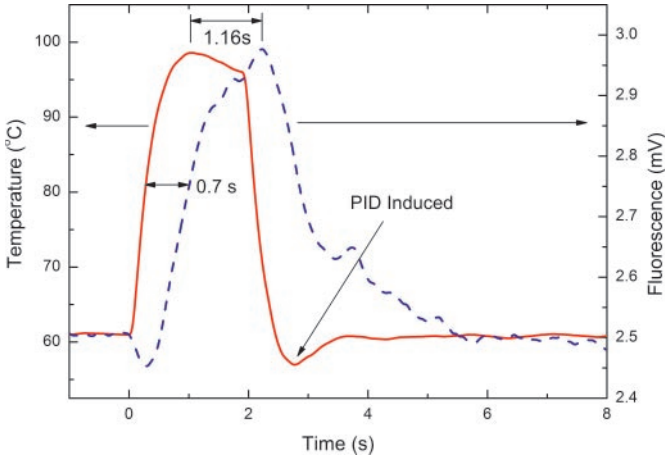

Figure 5. One thermal step of a PCR system. The red line represents temperature while the blue line represents fluorescence intensity, which is temperature-dependent. This graph shows that heat transfer from the heater to the sample is delayed by 1.16 s. The peak fluorescent intensity is achieved 2 s from the beginning of the heat pulse. The 'dip' in the temperature curve (indicated by an arrow 'PID induced') is caused by the PID based feedback loop. The glass cover slip served as a thermal separator, which slowed down the thermal energy transfer between the heater and the sample. Due to this effect the sharp peaks, seen in the temperature signals due to PID operation, were not visible in the fluorescent signal.

that up to 90°C, its fluorescence amplitude is proportional to its temperature. We have thus decided to use its fluorescence to estimate the PCR sample temperature.

By overlapping the temperature and fluorescent signals from the real-time PCR, we found that the delay between peak temperature and fluorescence signals (see Figure 5) is about 1.16 s. We can conclude that the recommended time of 3 s for denaturation according to the protocol for a conventional thermocycler can be shortened. After conducting a series of experiments, using the C_T value as a criterion for the PCR efficiency, we have observed that 2 s is indeed the shortest time for the denaturation without affecting the efficiency of the PCR. This time was then used throughout the experiments.

Our effort to optimize the PCR was then focused on annealing/extension time. As stated earlier, the amplitude of the fluorescent signal is proportional to the PCR product concentration. Looking at details of the fluorescent signal as a function of time starting from the 24th step onwards (see bottom Figure 4) the fluorescent signal in each cycle could be described by the equation:

$$F = A_0[1 - e^{(t-t_0)/\tau}] + A_1, \quad \mathbf{4}$$

where, A_0 is total signal increase during a single PCR step, A_1 is the starting amplitude of the fluorescence, t is time, t_0 is the starting time for the particular cycle, and τ is the PCR step time constant.

Once the annealing/extension time is longer than approximately three times the time constant, the product concentration is considered not to be changing anymore for a particular cycle. As the PCR amplification occurs only during the exponential part which, is only a marginal portion of the whole cycle (see Figure 4), the annealing/extension period could be significantly shortened to reduce the duration of the saturated region without affecting the PCR.

Analyzing the behavior of the time constant, we have found that it is linearly proportional to the cycle number N based on the formula:

$$\tau = -20.56 + 0.94*N, \quad \mathbf{5}$$

The time-constant relationship with the cycle number is probably related to the diffusion of the PCR chemicals.

With each subsequent cycle the amount of PCR product doubles (assuming 100% efficiency) and the demand for reagents grows with each cycle. We can speculate that at the beginning of the PCR/onset of the exponential growth primers, nucleotides (dNTPs), FAM and the enzyme are in excess, but continuously reduced by incorporation/synthesis of complementary strands. They are also partly denaturized by thermal stress and it would probably also affect the rate constant while the PCR progresses. However, besides this there are still dye-related issues such as, bleaching, optically and thermally, and the ratio of intact/lysed dye, dependence of the quantum yield of the dye from the buffer, especially ionic strength, which could increase because of evaporation.

We believe that the formula (4) can be used to derive the C_T value from the reaction as long as the cycle times are long enough to detect the exponential behavior. In this particular case, the value of N for τ to be equal zero is 21.9, which is comparable with the value of 20.8 derived using a standard way.

Beside the determination of a C_T value, the formula (4) contains another interesting part, such as the slope. It provides the information that the time constant of the PCR increases by 0.94 s per cycle. We assume that this number shows the rate of the depletion of reagents. Based on the assumption above we can speculate that by choosing the reagents, this time-constant variation with the cycle number can be also used to derive the PCR efficiency. If this speculation is correct, the PCR efficiency could then be calculated from a single measurement. However, it requires an extensive study using different reagent concentrations which is not the subject of this paper.

Real-time PCR results

As a benchmark we have carried out the recommended protocol as described earlier consisting of a hot start followed by 40 cycles using a commercial ABI 7500 PCR system. The C_T value obtained from the Light Cycler was 21, which is in good agreement with results obtained form the micro PCR system with annealing/elongation of 20 s. We can conclude that the performance of both systems is comparable.

Derivation of C_T values

First, the average amplitude of the fluorescence signal at the end of each annealing/elongation step was extracted (18) by our own program, normalized, and plotted as a function of the cycle number (see Figure 6A).

The standard methods for C_T derivation as well as the method proposed earlier in this paper could not be used for short annealing/elongation intervals. Once the annealing/elongation time is shorter than the value of time-constant τ

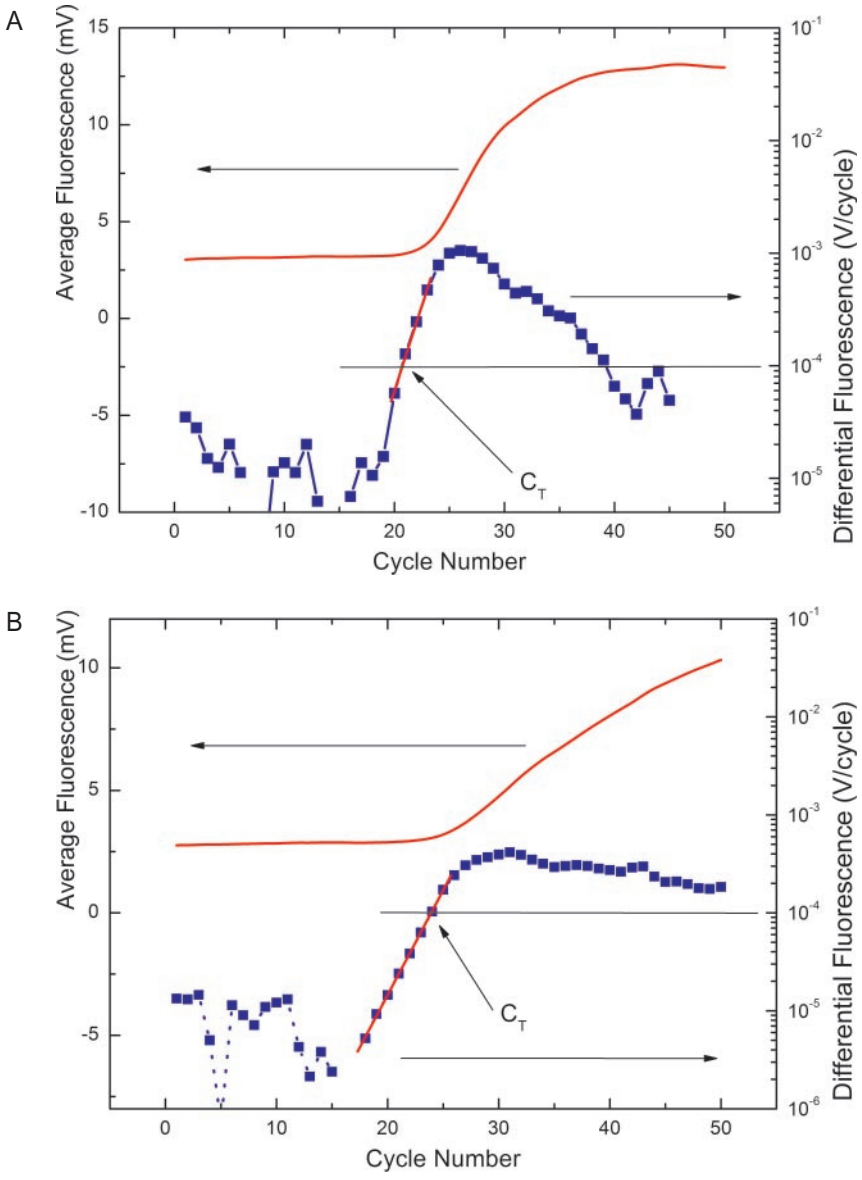

Figure 6. (**A**) Average fluorescence amplitude (red) and its differential value (blue) versus cycle number for an annealing/ elongation time of 15 s. The C_T value was derived as the most probable value of cycle number for the differential fluorescence of 10^{-4} mV as described in the text. This value was extracted by linear regression of the curve (blue) from its linear part. The value of C_T is indicated by an arrow. (**B**) The average fluorescence amplitude (red) and its differential value (blue) versus cycle number for an annealing/ elongation time of 5 s. Note the different profile with the respect to (A) of the fluorescence versus cycle number, where the typical saturation region is missing.

three times (see Figure 4 and Equation 4), the growth in fluorescence intensity does not follow an exponential pattern and the conventional way of data extraction is then no longer applicable. We have modified the conventional method by extracting the C_T value from a cross-section of the differential fluorescence (plotted on a logarithmic scale) with an arbitrary threshold value. It was found that this method is suitable for all PCR curves we have obtained.

Two typical samples of PCR curves for annealing/ elongation period longer (Figure 6A) and shorter (Figure 6B) than τ are shown here. The C_T values were extracted from differential fluorescence as described above and plotted versus annealing/ elongation time (see Figure 7). As long as the duration of the annealing/ elongation period was longer or equal to 10 s, the C_T remained unchanged with a value of 20.7 ± 0.2.

Once the annealing/ elongation time was between 6.5 and 9 s, the average C_T value grew to 21.7. This suggested that the efficiency of the PCR is not as high as before with respect to the benchmark measurement. Nevertheless, it is still acceptable for most experiments. The PCR efficiency reduction as a function of the C_T value could be described by the formula:

$$B = A^{C_{T1}/C_{T2}}, \qquad \mathbf{6}$$

where, A and B are PCR relative efficiencies related to critical threshold C_{T1} and C_{T2}, respectively.

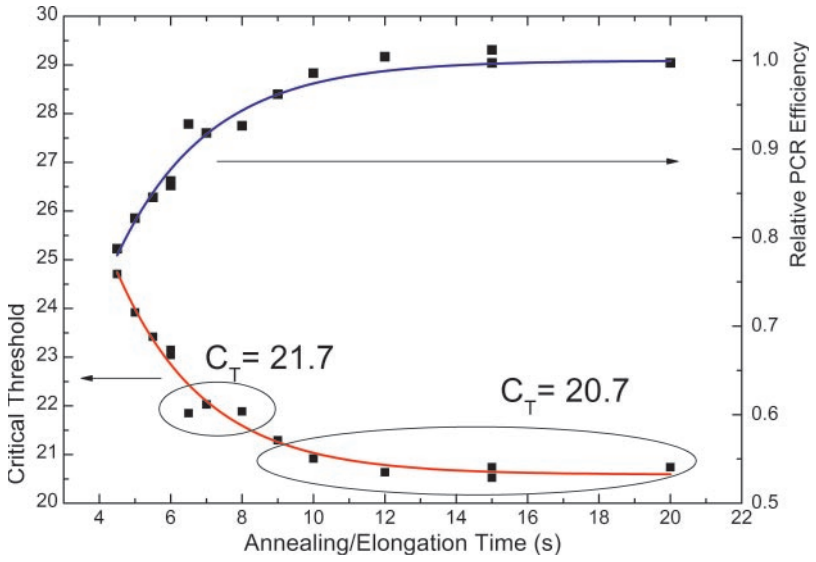

Figure 7. The C_T value as a function of annealing/ elongation time is shown in red. This demonstrated that the Taqman PCR system can be run with an annealing/ elongation step of 10 s. Even with this step as short as 6.5 s, the PCR performance is not significantly affected. This PCR system is then capable of running a complete 50 cycle PCR protocol in 7 min and 25 s inclusive of a 20 s hot start.

The relative PCR efficiency with respect to the efficiency A with a long annealing/ elongation time is shown in Figure 7 demonstrating that the annealing/ elongation time can be as short as 8 s without compromising the PCR performance. Once it is shorter than 6.5 s, the PCR efficiency dropped to 80% of the original efficiency value and the C_T grew to above 25.

DISCUSSION

As the PCR heating/ cooling rate is over 100°C s^{-1}, the PCR system is capable of completing a single cycle within 8.5 s, consisting of 2 s for denaturation and 6.5 s for annealing/ extension. The cycle time is probably still limited by the heat transfer from the heater to the PCR sample.

The optical setup for fluorescence detection was designed for one sample per analysis. We are currently developing a parallel system to run four PCRs simultaneously. The mercury lamp is replaced by a 490 nm light emitting diode (LED) and the PMT by a photodiode. A system with more than four PCRs at a time would probably require either multiple PMTs, photodiodes or a charge-coupled device (CCD).

We believe that the maximum number of PCR systems running in parallel made by the above-described technique might be between 10 and 20. Making a PCR system based on a similar micromachined silicon chip with more than 20 U working in parallel would require either a few micromachined silicon chips next to each other or one large silicon chip.

CONCLUSION

We have demonstrated, fabricated and tested a real-time PCR device with a heating rate of 175°C s^{-1} and a cooling rate of −125°C s^{-1}. The device itself requires only 0.2 s to heat up from 60 to 94°C and 0.27 s to cool back to 60°C. The heat transfer from the PCR system to the sample with a volume of 0.1 µl and covered with 1.1 µl of mineral oil requires about a second for heat transfer. Due to the fast transition time as well as the short time necessary for denaturation, the PCR performance is still mostly determined by the heat transfer and enzyme kinetics during annealing/ extension period. We have tested different thermal protocols in order to minimize the time necessary for the PCR. The shortest time achieved without compromising the process efficiency was 2 s for denaturation and 6.5 s for annealing/ extension. That corresponds to merely 5 min and 40 s required to complete 40 cycles of PCR.

Two alternative methods for C_T value extraction were proposed and tested. A method for PCR efficiency was also proposed.

ACKNOWLEDGEMENTS

The authors would like to thank our coworker Wanxin Sun for writing the Fortran program to extract the PCR fluorescent data, Vitek Zahlava for the PCB design and Tseng-Ming Hsieh for the original LabView program. The authors are also grateful to the Institute of Bioengineering and Nanotechnology, Singapore as well as the Agency for Science, Technology and Research, Singapore for their financial support. Besides that, the authors would also like to thank two anonymous reviewers who by very valuable comments help to improve quality of their paper. Funding to pay the Open Access publication charges for this article was provided by IBN.

Conflict of interest statement. None declared.

REFERENCES

1. Saiki,R.K., Scharf,S., Faloona,F., Mullis,K.B., Horn,G.T., Erlich,H.A. and Arnheim,N. (1985) Enzymatic amplification of beta-globin

genomic sequences and restriction site analysis for diagnosis of sickle-cell anemia. *Science*, **230**, 1350–1354.
2. Mullis,K.B., Feree,F. and Gibbs,R.A. (1994) *Polymerase Chain Reaction*. Binkhauser, Boston.
3. Saiki,R.K., Gelfand,D.H., Stoffel,S., Scharf,S., Higuchi,R., Horn,G.T., Mullis,K.B. and Erlich,H.A. (1988) Primer-directed enzymatic amplification of DNA with a thermostable DNA polymerase. *Science*, **239**, 487–491.
4. Cheng,J., Shoffner,M.A., Mitchelson,K.R., Kricka,L.J. and Wilding,P. (1996) Analysis of ligase chain reaction products amplified in a silicon-glass chip using capillary electrophoresis. *J. Chromatography A*, **732**, 151–158.
5. Lee,L.G., Connell,C.R. and Bloch,W. (1993) Allelic discrimination by nick-translation PCR with fluorogenic probes. *Nucleic Acids Res.*, **21**, 3761–3766.
6. Kubista,M., Andrade,J.M., Bengtsson,M., Forootan,A., Jonak,J., Lind,K., Sindelka,R., Sjoback,R., Sjogreen,B. and Strombom,L. (2006) The real-time polymerase chain reaction. *Mol. Aspects Med.*, **27**, 95–125.
7. Fixman,M. and Freire,J.J. (1977) Theory of DNA melting curves. *Biopolymers*, **16**, 2693–2704.
8. Rutledge,R.G. (2004) Sigmoidal curve-fitting redefines quantitative real-time PCR with the prospective of developing automated high-throughput. *Nucleic Acids Res.*, **32**, e178.
9. Petersen,K.E. (1982) Silicon as a mechanical material. *Proc. IEEE*, **70**, 420–457.
10. Grayson,A.C.R., Shawgo,R.S., Johnson,A.M., Flynn,N.T., Li,Y., Cima,M.J. and Langer,R. (2004) A BioMEMS review: MEMS technology for physiologically integrated devices. *Proc. IEEE*, **92**, 6–21.
11. Northrup,M.A., Bennet,B., Hadley,D., Landre,P., Lehew,S., Richards,J. and Stratton,P. (1998) A miniature analytical instrument for nucleic acids based on micromachined silicon reaction chambers. *Anal. Chem.*, **70**, 918–922.
12. Huhmer,A.F.R. and Landers,J.P. (2000) Infrared-mediated thermocycling for effective polymerase chain reaction amplification of DNA in nanoliter volume. *Anal. Chem.*, **72**, 5507–5512.
13. Kopp,M.U., de Mello,A.J. and Manz,A. (1998) Chemical amplification: continuous-flow PCR on a chip. *Science*, **280**, 1046–1048.
14. Liu,J., Enzelberger,M. and Quake,S. (2002) A nanoliter rotary device for polymerase chain reaction. *Electrophoresis*, **23**, 1531–1536.
15. Roper,M.G., Easley,C.J. and Landers,J.P. (2005) Advances in polymerase chain reaction on microfludic chip. *Anal. Chem.*, **77**, 3887–3894.
16. Giordano,B.C., Ferrance,J., Swedberg,S., Huhmer,A.F.R. and Landers,J.P. (2001) Polymerase chain reaction in polymeric microchips: DNA amplification in less than 240 seconds. *Anal. Biochem.*, **291**, 124–132.
17. Matsubara,Y., Kerman,K., Kobayashi,M., Yamamura,S., Morita,Y., Takamura,Y. and Tamiya,E. (2004) On-chip nanoliter-volume multiplex TaqMan polymerase chain reaction from a single copy based on counting fluorescence released microchambers. *Anal. Chem.*, **76**, 6434–6439.
18. Neuzil,P., Hsieh,T.-M. and Pipper,J. (2006) Disposable real-time microPCR device: lab-on-a-chip for few pennies, accepted for publication in *Molecular BioSystems*.
19. Neuzil,P. and Mei,T. (2002) Evaluation of thermal parameters of bolometer devices. *Appl. Phys. Lett.*, **80**, 1838–1840.
20. Laermer,F. and Schilp,A. (1996) Method for anisotropic plasma etching of substrates. *US patent 5498312*.
21. Zhuo,L., Sun,B., Zhang,C.L., Fine,A., Chiu,S.Y. and Messing,A. (1997) Live astrocytes visualized by green fluorescent protein in transgenic mice. *Dev. Biol.*, **187**, 36–42.
22. Nygren,J., Svanvik,N. and Kubista,M. (1998) The interactions between the fluorescent dye thiazole orange and DNA. *Biopolymers*, **46**, 39–51.